

On the temporal discretizations of convection dominated convection-diffusion equations in time-dependent domain

*Shweta Srivastava*¹, *Sashikumaar Ganesan*²

May, 2018

Abstract

This paper presents the numerical analysis of a convection dominated scalar equation with different time discretizations in time-dependent domains. The implicit Euler, Crank-Nicolson and backward-difference methods are used for the temporal discretization. The time-dependent domain is handled by the arbitrary Lagrangian-Eulerian (ALE) approach. In particular, the non-conservative form of the ALE scheme is considered. The Streamline Upwind Petrov-Galerkin (SUPG) finite element method is used for spatial discretization. It is shown that the stability of the fully discrete solution, irrespective of the temporal discretization, is only conditionally stable. The dependence of the numerical solution on the stabilization parameter δ_k is also studied. It is seen that the Crank-Nicolson scheme is less dissipative than the implicit Euler and the backward difference method. Moreover, the backward difference scheme is more sensitive to the stabilization parameter δ_k than the other time discretizations.

MSC(2010): 35Q35, 65M12, 65M60.

Keywords: Convection-diffusion-reaction equation, SUPG stabilization, Geometric conservation Law (GCL), time-dependent domain, arbitrary Lagrangian-Eulerian approach, temporal discretizations.

¹ *IISc Mathematics Initiative (IMI), Department of Mathematics, Indian Institute of Science (IISc), Bangalore, India.*

² *Department of Computational and Data Sciences, Indian Institute of Science (IISc), Bangalore, India.*

1 Introduction

Solution of a transient convection-diffusion-reaction equation in a time-dependent domain is highly demanded in many applications. The scalar variable can be a temperature or a concentration or a density of a species. Numerical approximation of the solution of a scalar partial differential equation becomes more challenging when the equation is convection dominated. Further, the computations become more complex when the domain contains moving boundaries, e.g., fluid-structure interactions (FSI) problems. In addition to a stabilized numerical method, an efficient approach is necessary to handle the mesh movement in time-dependent domains.

In general, the standard Galerkin finite element approximation induces spurious oscillations in the numerical solution of a convection dominated convection-diffusion equation. Therefore, stabilization schemes, as for instance, the streamline upwind Petrov-Galerkin (SUPG) [1, 3, 19], the local projection stabilization [11, 7], the continuous interior penalty method [4, 5], the subgrid scale modeling [8], the orthogonal subscales method [12, 13], have been proposed and analyzed in the literature. Each of these methods has its own advantages and disadvantages. Nevertheless, almost all stabilization methods introduce an unknown numerical parameter that controls the stability. The optimal choice of this parameter is an open problem [10, 19, 15, 16]. Almost all these stabilization methods have been studied only for PDEs in stationary domains.

In this paper, the SUPG finite element scheme for the computation of transient convection-diffusion equation in time-dependent domains is presented. Further, the arbitrary Lagrangian-Eulerian (ALE) approach is used to handle the moving boundaries of the time-dependent domain. The ALE formulation introduces a convection type mesh velocity term into the model equation, and hence it alters the overall convective field of the problem. Nevertheless, the model problem can still be convection dominated and can have boundary/interior layers even after reformulating into an ALE form.

Conservative and non-conservative forms are the two variants of the ALE approach. The stability estimates for the conservative ALE-SUPG discretization with the backward Euler and the Crank-Nicolson methods have been derived in [14]. In this paper, we consider the non-conservative ALE form. Further, backward Euler, Crank-Nicolson, and backward difference (BDF2) methods are considered for the temporal discretization. The non-conservative ALE-SUPG formulation avoids the necessity of the geometric conservation law (GCL). As it has been discussed in [6], GCL mainly boils down to a quadrature formula for the exact time integration of the term containing the mesh velocity introduced from Reynolds identity. Though we considered the non-conservative form, and the GCL is not needed, still we get only the conditionally stable estimates, which reflects the issue with the numerical computation of mesh velocity term \mathbf{w} in the analysis. The stability estimates for the implicit Euler, Crank-Nicolson, and backward difference time discretizations with inconsistent SUPG for non-conservative ALE form of the convection-diffusion-reaction equation in time-dependent domains are derived. It can be seen from the numerical results that the behavior of the solutions of conservative and non-conservative ALE forms depends on the deformation of the domain. If the deformation of the domain or the mesh velocity is large, the solution is very much influenced by the ALE form. Contrarily, the difference between the solutions of different ALE forms is almost negligible when the deformation of the domain is small.

The paper is organized as follows. In Section 2, transient convection-diffusion equation in a time-dependent domain and its ALE formulation are given. The spatial discretization using the SUPG finite element method is also presented in this section. Further, the stability of the semi-discrete (in space) problem is derived. Section 3 is devoted to the stability estimates of the fully discrete problem with implicit Euler, Crank-Nicolson, and backward difference (BDF2) discretization in time. Numerical results are presented in Section 4. Finally, a brief summary is presented in Section 5.

2 Statement of the problem

Let Ω_t be a time-dependent bounded domain in R^d , $d = 2, 3$, with Lipschitz boundary $\partial\Omega_t$ for each $t \in [0, T]$. Here, T is a given end time. Consider a transient convection-diffusion-reaction equation: find $u(t, x) : (0, T] \times \Omega \rightarrow \mathbb{R}$ subject to

$$\begin{aligned} \frac{\partial u}{\partial t} - \epsilon \Delta u + \mathbf{b} \cdot \nabla u + cu &= f && \text{in } (0, T] \times \Omega_t, \\ u &= 0 && \text{on } [0, T] \times \partial\Omega_t, \\ u(0, x) &= u_0(x) && \text{in } \Omega_0. \end{aligned} \quad (2.1)$$

Here $u(t, x)$ is an unknown scalar function, $u_0(x)$ is a given initial data, ϵ is the diffusivity constant, $\mathbf{b}(t, x)$ is the convective flow velocity, $c(t, x)$ is a reaction function, and $f(x)$ is a given source term with $f \in L^2(\Omega_t)$.

2.1 ALE formulation

Let $\hat{\Omega}$ be a reference domain. The reference domain $\hat{\Omega}$ can simply be the initial domain Ω_0 or the previous time-step domain when the deformation of the domain is large. Let \mathcal{A}_t be a family of bijective ALE mappings, which, at each time $t \in (0, T]$, maps a point Y of a reference domain $\hat{\Omega}$ to a point on the current domain Ω_t , given by

$$\mathcal{A}_t : \hat{\Omega} \rightarrow \Omega_t, \quad \mathcal{A}_t(Y) = x(Y, t), \quad t \in (0, T).$$

Further, for any time $t_1, t_2 \in [0, T]$, the ALE mapping between two time levels will be given by

$$\mathcal{A} : \Omega_{t_1} \rightarrow \Omega_{t_2} \quad \mathcal{A}_{t_1, t_2} = \mathcal{A}_{t_2} \circ \mathcal{A}_{t_1}^{-1}.$$

We assume that Ω_t is bounded with Lipschitz continuous boundary for each $t \in [0, T]$. For a function $g \in C^0(\Omega_t)$ on the Eulerian frame, we define the corresponding function $\hat{g} \in C^0(\hat{\Omega})$ on the ALE frame as

$$\hat{g} : \hat{\Omega} \times (0, T) \rightarrow \mathbb{R}, \quad \hat{g} = g \circ \mathcal{A}_t, \quad \text{with} \quad \hat{g}(Y, t) = g(\mathcal{A}_t(Y), t).$$

The temporal derivative on the ALE frame is defined as

$$\frac{\partial g}{\partial t} \Big|_Y : \Omega_t \times (0, T) \rightarrow \mathbb{R}, \quad \frac{\partial g}{\partial t} \Big|_Y(x, t) = \frac{\partial \hat{g}}{\partial t}(Y, t), \quad Y = \mathcal{A}_t^{-1}(x).$$

We apply the chain rule to the time derivative of $g \circ \mathcal{A}_t$ on the ALE frame to get

$$\frac{\partial g}{\partial t} \Big|_Y = \frac{\partial g}{\partial t}(x, t) + \frac{\partial x}{\partial t} \Big|_Y \cdot \nabla_x g = \frac{\partial g}{\partial t} + \frac{\partial \mathcal{A}_t(Y)}{\partial t} \cdot \nabla_x g = \frac{\partial g}{\partial t} + \mathbf{w} \cdot \nabla_x g,$$

where the domain velocity \mathbf{w} is defined as

$$\mathbf{w}(x, t) = \frac{\partial x}{\partial t} \Big|_Y(\mathcal{A}_t^{-1}(x), t).$$

By using the relation in the model problem (2.1), we get

$$\frac{\partial u}{\partial t} \Big|_Y - \epsilon \Delta u + (\mathbf{b} - \mathbf{w}) \cdot \nabla u + cu = f. \quad (2.2)$$

This equation is the ALE counterpart of the model equation (2.1). The difference between equations (2.1) and (2.2) is the additional domain velocity in the ALE form that accounts for the deformation of the domain.

2.2 Variational form

In this section, the finite element variational form of the ALE equation (2.2) is derived. Let

$$V = \left\{ v \in H_0^1(\Omega_t), \quad v : \Omega_t \times (0, T] \rightarrow \mathbb{R}, \quad v = \hat{v} \circ \mathcal{A}_t^{-1}, \quad \hat{v} \in H_0^1(\hat{\Omega}) \right\}$$

be the solution space for equation (2.2). Multiplying equation (2.2) with a test function $v \in V$ and applying integration by parts to the higher order derivative term, the variational form of the equation (2.2) becomes: find $u \in V$ such that

$$\left(\frac{\partial u}{\partial t} \Big|_Y, v \right) + (\epsilon \nabla u, \nabla v) + ((\mathbf{b} - \mathbf{w}) \cdot \nabla u, v) + (cu, v) = (f, v), \quad v \in V, \quad (2.3)$$

for given \mathbf{b} , \mathbf{w} , c , u_0 , Ω_0 , f , and for all $t \in (0, T]$. Of course, (\cdot, \cdot) denotes the L^2 -inner product in Ω_t .

Further, the notations for L^2 -inner product, the norm and the seminorm, $(\cdot, \cdot)_t$, $\|\cdot\|_{0,t}$ and $|\cdot|_{1,t}$, respectively over Ω_t , which will be followed throughout the paper, are given as

$$(u, v)_t = \int_{\Omega_t} uv \, dx, \quad \|v\|_{0,t}^2 = (v, v)_t, \quad |v|_{1,t}^2 = (\nabla v, \nabla v)_t, \quad \text{for } u, v \in V.$$

2.3 SUPG finite element space discretization

The numerical analysis for the standard Galerkin solution of (2.3) can be found in [2, 6, 9]. It has been shown that the stability estimate is independent of the domain velocity. However, the Galerkin approximation suffers instabilities for convection dominant scalar equations of type (2.3). In order to overcome this issue, we use the SUPG stabilization for the considered model problem with ALE equation (2.3). Note that the convective velocity in the ALE form is “ $(\mathbf{b} - \mathbf{w})$ ”, whereas the convective velocity for problems in time-independent domains is “ \mathbf{b} ”.

Let $\mathcal{T}_{h,0}$ be a triangulation of the domain Ω_0 . For each $t \in (0, T]$, $\mathcal{T}_{h,t}$ denote the family of shape regular triangulations of Ω_t into simplices obtained by triangulating the time-dependent domain Ω_t . We denote the diameter of the cell $K \in \mathcal{T}_{h,t}$ by $h_{K,t}$ and the global mesh size in the triangulated domain $\Omega_{h,t}$ by $h_t = \max\{h_{K,t} : K \in \mathcal{T}_{h,t}\}$. Suppose $V_h \subset V$ is a conforming finite element (finite dimensional) space. Let $\phi_h = \phi_i(x)$, $i = 1, 2, \dots, \mathcal{N}$, be the finite element basis functions of V_h . The discrete finite element space V_h is then defined by

$$V_h = \{v_h \in C(\overline{\Omega_t}) : v_h|_{\partial\Omega_t} = 0; v_h|_K \in P_k(K)\} \subset H_0^1(\Omega_t),$$

where P_k is the set of polynomials of degree less than or equal to k for discretization of the ALE mapping in space. We next define the discrete ALE mapping $\mathcal{A}_{h,t}(Y)$ and the mesh velocity \mathbf{w}_h in space. We use the Lagrangian finite element space

$$\mathcal{L}^k(\hat{\Omega}) = \left\{ \psi \in H^k(\hat{\Omega}) : \psi|_{\hat{K}} \in P_k(\hat{K}) \text{ for all } \hat{K} \in \hat{\Omega}_h \right\},$$

Using the linear space, we define the semidiscrete ALE mapping in space for each $t \in [0, T]$ by

$$\mathcal{A}_{h,t} : \hat{\Omega}_h \rightarrow \Omega_{h,t}. \quad (2.4)$$

Further, the semidiscrete (continuous in time) mesh velocity $\mathbf{w}_h(t, Y) \in \mathcal{L}^1(\hat{\Omega})^d$ in the ALE frame for each $t \in [0, T]$ is defined by

$$\hat{\mathbf{w}}_h(t, Y) = \sum_{i=1}^{\mathcal{M}} \mathbf{w}_i(t) \psi_i(Y); \quad \mathbf{w}_i(t) \in \mathbb{R}^d.$$

Here $\mathbf{w}_i(t)$ denotes the mesh velocity of the i^{th} node of simplices at time t , and $\psi_i(Y)$, $i = 1, 2, \dots, \mathcal{M}$, are the basis functions of $\mathcal{L}^1(\hat{\Omega}_h)$. We then define the semidiscrete mesh velocity in the Eulerian frame as

$$\mathbf{w}_h(t, x) = \hat{\mathbf{w}}_h \circ \mathcal{A}_{h,t}^{-1}(x).$$

Using the above finite element spaces and applying the inconsistent SUPG finite element discretization to the ALE form (2.2), the semidiscrete form in space reads as follows. For a given $u_h(x, 0) = u_{h,0}$, \mathbf{b} , \mathbf{w}_h , c , $\Omega_{h,0}$ and f , find $u_h(t, x) \in V_h$ such that, for all $t \in (0, T]$, we have

$$\begin{aligned} \left(\frac{\partial u_h}{\partial t} \Big|_Y, v_h \right)_t + a_{SUPG}(u_h, v_h)_t - \int_{\Omega_{h,t}} \mathbf{w}_h \cdot \nabla u_h v_h dx = \\ = \int_{\Omega_{h,t}} f v_h dx + \sum_{K \in \mathcal{T}_{h,t}} \delta_K \int_K f (\mathbf{b} - \mathbf{w}_h) \cdot \nabla v_h dK, \end{aligned} \quad (2.5)$$

where

$$\begin{aligned} a_{SUPG}(u, v)_t = \epsilon(\nabla u, \nabla v)_t + (\mathbf{b} \cdot \nabla u, v)_t + (cu, v)_t + \\ + \sum_{K \in \mathcal{T}_{h,t}} \delta_K (-\epsilon \Delta u + (\mathbf{b} - \mathbf{w}_h) \cdot \nabla u + cu, (\mathbf{b} - \mathbf{w}_h) \cdot \nabla v)_K. \end{aligned} \quad (2.6)$$

Here δ_K is the local stabilization parameter, whose value depends on the mesh size and the convective velocity field. Further, $u_{h,0} \in V_h$ is defined as the L^2 -projection of the initial value u_0 onto V_h .

Next we briefly describe the inverse inequality used in our subsequent analysis, given as

$$\|\Delta u_h\|_{0,K} = c_{inv} h_K^{-1} |u_h|_{1,K}, \quad \text{for all } u_h \in V_h, \quad (2.7)$$

where c_{inv} is a constant.

Lemma 1. Coercivity of $a_{SUPG}(\cdot, \cdot)$: Assume that there exists a constant μ such that

$$\left(c - \frac{1}{2} \nabla \cdot \mathbf{b} \right) (x) \geq \mu > 0, \quad \text{for all } x \in \Omega_t. \quad (2.8)$$

Let the discrete form of assumption (2.8) be satisfied. Assume that the SUPG parameter satisfies

$$\delta_K \leq \frac{\mu}{2 \|c\|_{K,\infty}^2}, \quad \delta_K \leq \frac{h_K^2}{2 \epsilon c_{inv}^2}, \quad (2.9)$$

where c_{inv} is a constant used in the inverse inequality; see equation (2.7). Then, the SUPG bilinear form satisfies

$$a_{SUPG}(u_h, u_h)_t \geq \frac{1}{2} \| \|u_h\| \|_t^2,$$

where the mesh dependent norm is defined as

$$\| \|u\| \|_t^2 = \left(\epsilon |u|_{1,t}^2 + \sum_{K \in \mathcal{T}_{h,t}} \delta_K \|(\mathbf{b} - \mathbf{w}_h) \cdot \nabla u\|_{0,K}^2 + \mu \|u\|_{0,t}^2 \right).$$

Proof. The coercivity of the bilinear form follows from [14, Lemma 1]. □

Lemma 2. Stability of the semi-discrete problem: Let the discrete version of (2.8) and the assumption (2.9) on δ_K hold true. Then, the

solution of problem (2.5) satisfies

$$\begin{aligned} \|u_h(t)\|_{0,t}^2 + \frac{1}{2} \int_0^T \|u_h(t)\|_t^2 dt &\leq \|u_h(0)\|_{0,t}^2 + \frac{2}{\mu} \int_0^T \|f(t)\|_{0,t}^2 dt \\ &\quad + 2 \int_0^T \sum_{K \in \mathcal{T}_{h,t}} \delta_K \|f(t)\|_{0,K}^2 dt. \end{aligned}$$

Proof. Take $v_h = u_h$ in equation (2.5) and consider the relations

$$\int_{\Omega_{h,t}} \frac{\partial u_h}{\partial t} \Big|_Y u_h dx = \frac{1}{2} \left(\frac{d}{dt} \|u_h\|_{0,t}^2 - \int_{\Omega_{h,t}} u_h^2 \nabla \cdot \mathbf{w}_h dx \right)$$

and

$$\int_{\Omega_{h,t}} \mathbf{w}_h \cdot \nabla u_h u_h dx = -\frac{1}{2} \int_{\Omega_{h,t}} u_h^2 \nabla \cdot \mathbf{w}_h dx.$$

Use the Cauchy-Schwarz inequality to bound the right hand side terms:

$$|(f, u_h)| = \left| \left(\frac{f}{\mu^{1/2}}, \mu^{1/2} u_h \right) \right| \leq \frac{1}{\mu} \|f\|_{0,t}^2 + \frac{1}{4} \mu \|u_h\|_{0,t}^2$$

and

$$\begin{aligned} \left| \sum_{K \in \mathcal{T}_{h,t}} \delta_K (f, (\mathbf{b} - \mathbf{w}_h) \cdot \nabla u_h)_K \right| &\leq \sum_{K \in \mathcal{T}_{h,t}} \delta_K \|f\|_{0,K}^2 + \\ &\quad \frac{1}{4} \sum_{K \in \mathcal{T}_{h,t}} \delta_K \|(\mathbf{b} - \mathbf{w}_h) \cdot \nabla u_h\|_{0,K}^2. \end{aligned}$$

Now with the coercivity of bilinear form, the stability estimate for the semi-discrete problem can be derived. Here the stability properties are not affected by the domain velocity field in the semi-discrete problem (2.5). However, we may not expect the same result to hold true for the fully discrete case. \square

3 Fully discrete scheme

In this section the stability estimates for the fully discrete ALE-SUPG form are derived. We consider the first order implicit Euler, the second order modified Crank-Nicolson, and the backward-difference (BDF2) method for the temporal discretization.

Consider the partition of the time interval $[0, T]$ as $0 = t^0 < t^1 < \dots < t^N = T$ into N equal sub-intervals. Let us denote the uniform time step by $\Delta t = \tau^n = t^n - t^{n-1}$, $1 \leq n \leq N$. Further, let u_h^n be the approximation of $u(t^n, x)$ in $V_h \subset H_0^1(\Omega_{t^n})$, where Ω_{t^n} is the deforming domain at time $t = t^n$.

We first discretize the ALE mapping in time using a linear interpolation. We denote the discrete ALE mapping by $\mathcal{A}_{h, \Delta t}$, and define it for every $\tau \in [t^n, t^{n+1}]$ by

$$\mathcal{A}_{h, \Delta t}(Y) = \frac{\tau - t^n}{\Delta t} \mathcal{A}_{h, t^{n+1}}(Y) + \frac{t^{n+1} - \tau}{\Delta t} \mathcal{A}_{h, t^n}(Y),$$

where $\mathcal{A}_{h, t}(Y)$ is the time continuous ALE mapping exhibited in (2.4). Since the ALE mapping is discretized in time using a linear interpolation, we obtain the discrete mesh velocity

$$\hat{\mathbf{w}}_h^{n+1}(Y) = \frac{\mathcal{A}_{h, t^{n+1}}(Y) - \mathcal{A}_{h, t^n}(Y)}{\Delta t} = \frac{x_h^{n+1} - x_h^n}{\Delta t} \quad (3.1)$$

as a piecewise constant function in time. We define the mesh velocity on the Eulerian frame as

$$\mathbf{w}_h^{n+1} = \hat{\mathbf{w}}_h^{n+1} \circ \mathcal{A}_{h, \Delta t}^{-1}(x).$$

Further, the integral u_h^n on a domain Ω_{t^s} , with $t^s \neq t^n$, is written through the ALE mapping as

$$\int_{\Omega_{t^s}} u_h^n dX = \int_{\Omega_{t^s}} u_h^n \circ \mathcal{A}_{t^n, t^s} dX.$$

3.1 Discrete ALE-SUPG with implicit Euler time discretization method

Applying the backward Euler time discretization to the semi-discrete problem (2.5), the discrete form reads

$$\begin{aligned} & \left(\frac{u_h^{n+1} - u_h^n}{\Delta t}, v_h \right)_{t^{n+1}} + a_{SUPG}^{n+1}(u_h^{n+1}, v_h)_t - \int_{\Omega_{t^{n+1}}} \mathbf{w}_h^{n+1} \cdot \nabla u_h^{n+1} v_h \, dx \\ & = \int_{\Omega_{t^{n+1}}} f^{n+1} v_h \, dx + \sum_{K \in \mathcal{T}_{h,t^{n+1}}} \delta_K \int_K f^{n+1} (\mathbf{b} - \mathbf{w}_h^{n+1}) \cdot \nabla v_h \, dK, \end{aligned} \tag{3.2}$$

where

$$\begin{aligned} a_{SUPG}^{n+1}(u_h, v_h) & = \epsilon(\nabla u_h, \nabla v_h)_{t^{n+1}} + (\mathbf{b} \cdot \nabla u_h, v_h)_{t^{n+1}} + (cu_h, v_h)_{t^{n+1}} + \\ & \sum_{K \in \mathcal{T}_{h,t^{n+1}}} \delta_K (-\epsilon \Delta u_h + (\mathbf{b} - \mathbf{w}_h^{n+1}) \cdot \nabla u_h + cu_h, (\mathbf{b} - \mathbf{w}_h^{n+1}) \cdot \nabla v_h)_K. \end{aligned}$$

Lemma 3. Stability estimate for non-conservative ALE-SUPG form with implicit Euler method: *Let the discrete version of (2.8) and the assumption (2.9) on δ_K hold true. Further, assume $\delta_K \leq \frac{\Delta t}{4}$. Then the solution of problem (3.2) satisfies*

$$\begin{aligned} & \|u_h^{n+1}\|_{0,t^{n+1}}^2 + \frac{\Delta t}{2} \sum_{i=1}^{n+1} \|u_h^i(t)\|_{t^i}^2 \leq \\ & \leq \left((1 + \Delta t \alpha_2^0) \|u_h^0\|_{0,t^0}^2 + \Delta t \sum_{i=1}^{n+1} \left(\frac{2}{\mu} + \frac{\Delta t}{2} \right) \|f^i(t)\|_{0,t^i}^2 \right) \cdot \\ & \exp \left(\Delta t \sum_{i=1}^{n+1} \frac{\alpha_1^i + \alpha_2^i}{1 - \Delta t(\alpha_1^i + \alpha_2^i)} \right), \end{aligned}$$

where α_1^n and α_2^n are defined as in the proof of this lemma.

Proof. Substituting $v_h = u_h^{n+1}$ in the discrete form (3.2) and applying

integration by parts to the mesh velocity integral term, we get

$$\begin{aligned} & \left(\frac{u_h^{n+1} - u_h^n}{\Delta t}, u_h^{n+1} \right)_{t^{n+1}} + a_{SUPG}^{n+1}(u_h^{n+1}, u_h^{n+1}) + \frac{1}{2} \int_{\Omega_{t^{n+1}}} \nabla \cdot \mathbf{w}_h^{n+1} |u_h^{n+1}|^2 dx \\ &= \int_{\Omega_{t^{n+1}}} f^{n+1} u_h^{n+1} dx + \sum_{K \in \mathcal{T}_{t^{n+1}}} \delta_K \int_K f^{n+1} (\mathbf{b} - \mathbf{w}_h^{n+1}) \cdot \nabla u_h^{n+1} dK. \end{aligned}$$

Using the coercivity of the bilinear form a_{SUPG} , the Cauchy-Schwarz inequality yields

$$\begin{aligned} & \|u_h^{n+1}\|_{0,t^{n+1}}^2 + \frac{\Delta t}{2} \|u_h^{n+1}\|_{t^{n+1}}^2 \\ & \leq -\frac{1}{2} \Delta t \int_{\Omega_{t^{n+1}}} \nabla \cdot \mathbf{w}_h^{n+1} |u_h^{n+1}|^2 dx + \frac{1}{2} \|u_h^n\|_{0,t^{n+1}}^2 \\ & + \frac{1}{2} \|u_h^{n+1}\|_{0,t^{n+1}}^2 + \frac{\Delta t}{4} \sum_{K \in \mathcal{T}_{h,t^{n+1}}} \delta_K \|(\mathbf{b} - \mathbf{w}_h^{n+1}) \cdot \nabla u_h^{n+1}\|_{0,K}^2 \\ & + \Delta t \sum_{K \in \mathcal{T}_{h,t^{n+1}}} \delta_K \|f^{n+1}\|_{0,K}^2 + \frac{\Delta t}{\mu} \|f^{n+1}\|_{0,t^{n+1}}^2 + \Delta t \frac{\mu}{4} \|u_h^{n+1}\|_{0,t^{n+1}}^2. \end{aligned}$$

From the Reynolds identity, we have

$$\|u_h^n\|_{0,t^{n+1}}^2 = \|u_h^n\|_{0,t^n}^2 + \int_{t^n}^{t^{n+1}} \int_{\Omega_t} \nabla \cdot \mathbf{w}_h |u_h^n|^2 dx dt,$$

and we get

$$\begin{aligned} & \|u_h^{n+1}\|_{0,t^{n+1}}^2 + \frac{1}{2} \Delta t \|u_h^{n+1}\|_{t^{n+1}}^2 \leq \int_{t^n}^{t^{n+1}} \int_{\Omega_t} \nabla \cdot \mathbf{w}_h |u_h^n|^2 dx dt \\ & - \frac{\Delta t}{2} \int_{\Omega_{t^{n+1}}} \nabla \cdot \mathbf{w}_h^{n+1} |u_h^{n+1}|^2 dx + \|u_h^n\|_{0,t^n}^2 + \Delta t \frac{2}{\mu} \|f^{n+1}\|_{0,t^{n+1}}^2 \\ & + 2\Delta t \sum_{K \in \mathcal{T}_{h,t^{n+1}}} \delta_K \|f^{n+1}\|_{0,t^{n+1}}^2. \end{aligned}$$

Let

$$\mathcal{A}_{t_n, t_{n+1}} = \mathcal{A}_{t_{n+1}} \circ \mathcal{A}_{t_n}^{-1}$$

be the ALE mapping between Ω_{t^n} and $\Omega_{t^{n+1}}$, and $J_{\mathcal{A}_{t^n, t^{n+1}}}$ be its Jacobian. Then we have

$$\begin{aligned} & \|u_h^{n+1}\|_{0, t^{n+1}}^2 + \frac{1}{2} \Delta t \|u_h^{n+1}\|_{t^{n+1}}^2 \\ & \leq \Delta t \|\nabla \cdot \mathbf{w}_h(t^{n+1})\|_{\infty, t^{n+1}} \|u_h^{n+1}\|_{0, t^{n+1}}^2 + \Delta t \frac{2}{\mu} \|f^{n+1}\|_{0, t^{n+1}}^2 \\ & + \left(1 + \Delta t \sup_{t \in (t^n, t^{n+1})} \|J_{\mathcal{A}_{t^n, t^{n+1}}} \nabla \cdot \mathbf{w}_h\|_{\infty, t} \right) \|u_h^n\|_{0, t^n}^2 \\ & + \Delta t \sum_{K \in \mathcal{T}_{h, t^{n+1}}} \delta_K \|f^{n+1}\|_{0, t^{n+1}}^2. \end{aligned}$$

Further, using the notation

$$\begin{aligned} \alpha_1^n & = \|\nabla \cdot \mathbf{w}_h(t^n)\|_{\infty, t^n}, \\ \alpha_2^n & = \sup_{t \in (t^n, t^{n+1})} \|J_{\mathcal{A}_{t^n, t^{n+1}}} \nabla \cdot \mathbf{w}_h\|_{\infty, t}, \end{aligned}$$

the above equation can be written as

$$\begin{aligned} & \|u_h^{n+1}\|_{0, t^{n+1}}^2 + \frac{1}{2} \Delta t \|u_h^{n+1}\|_{t^{n+1}}^2 \leq \\ & \leq \Delta t \alpha_1^{n+1} \|u_h^{n+1}\|_{0, t^{n+1}}^2 + (1 + \Delta t \alpha_2^n) \|u_h^n\|_{0, t^n}^2 + \\ & \Delta t \frac{2}{\mu} \|f^{n+1}\|_{0, t^{n+1}}^2 + 2\Delta t \sum_{K \in \mathcal{T}_{h, t^{n+1}}} \delta_K \|f^{n+1}\|_{0, t^{n+1}}^2. \end{aligned}$$

Summing over the index as $i = 0, 1, 2, \dots, n$, and using the assumptions

on δ_K , we arrive to

$$\begin{aligned}
 & \|u_h^{n+1}\|_{0,t^{n+1}}^2 + \frac{1}{2}\Delta t \sum_{i=1}^{n+1} \|u_h^i(t)\|_{t^i}^2 \leq \\
 & \leq \Delta t \alpha_1^{n+1} \|u_h^{n+1}\|_{0,t^{n+1}}^2 + \Delta t \sum_{i=1}^n (\alpha_1^i + \alpha_2^i) \|u_h^i\|_{0,t^i}^2 + (1 + \Delta t \alpha_2^0) \|u_h^0\|_{0,t^0}^2 \\
 & \quad + 2\Delta t \sum_{i=1}^{n+1} \sum_{K \in \mathcal{T}_{h,t^i}} \delta_K \|f^n\|_{0,t^i}^2 + \Delta t \sum_{i=1}^{n+1} \frac{2}{\mu} \|f^i\|_{0,t^i}^2 \\
 & \leq \Delta t \sum_{i=1}^{n+1} (\alpha_1^i + \alpha_2^i) \|u_h^i\|_{0,t^i}^2 + (1 + \Delta t \alpha_2^0) \|u_h^0\|_{0,t^0}^2 \\
 & \quad + \sum_{i=1}^{n+1} \left(\frac{2\Delta t}{\mu} + \frac{\Delta t^2}{2} \right) \|f^i\|_{0,t^i}^2.
 \end{aligned}$$

We now apply Gronwall's lemma to get

$$\begin{aligned}
 & \|u_h^{n+1}\|_{0,t^{n+1}}^2 + \frac{\Delta t}{2} \sum_{i=1}^{n+1} \|u_h^i(t)\|_{t^i}^2 \leq \\
 & \leq \left[(1 + \Delta t \alpha_2^0) \|u_h^0\|_{0,t^0}^2 + \Delta t \sum_{i=1}^{n+1} \left(\frac{2}{\mu} + \frac{\Delta t}{2} \right) \|f^i\|_{0,t^i}^2 \right] \\
 & \quad \exp \left(\Delta t \sum_{i=1}^{n+1} \frac{\alpha_1^i + \alpha_2^i}{1 - \Delta t (\alpha_1^i + \alpha_2^i)} \right).
 \end{aligned}$$

The above stability estimate is stable provided we have

$$\Delta t < \frac{1}{\alpha_1^n + \alpha_2^n} = \left(\|\nabla \cdot \mathbf{w}_h(t^n)\|_{\infty,t^n} + \sup_{t \in (t^n, t^{n+1})} \|J_{A_{t^n, t^{n+1}}} \nabla \cdot \mathbf{w}_h\|_{\infty,t} \right)^{-1}$$

□

3.2 Discrete ALE-SUPG with Crank-Nicolson time discretization

We now consider the modified Crank-Nicolson method which is basically Runge-Kutta method of order two. For an equation

$$\frac{du(t)}{dt} = f(u(t), t), \quad t > 0 \quad \text{and} \quad u(0) = u_0, \quad (3.3)$$

with the modified Crank-Nicolson method, we get

$$u^{n+1} - u^n = \Delta t f \left(\frac{u^{n+1} + u^n}{2}, t^{n+\frac{1}{2}} \right).$$

Lemma 4. Stability estimates for the non-conservative ALE-SUPG form applying Crank-Nicolson method: *Let the discrete version of (2.8) and the assumption (2.9) on δ_K hold true. Further, assume $\delta_K \leq \frac{\Delta t}{4}$. Then the solution obtained from the Crank-Nicolson time discretization satisfies*

$$\begin{aligned} & \|u_h^{n+1}\|_{0,t^{n+1}}^2 + \frac{\Delta t}{4} \sum_{i=0}^n \|u_h^{i+1} + u_h^i\|_{t^{i+1/2}}^2 \leq \\ & \leq \left((1 + \Delta t \beta_2^0) \|u_h^0\|_{0,t^0}^2 + \Delta t \sum_{i=0}^n \left(\frac{2}{\mu} + \Delta t \right) \|f^{i+1/2}\|_{0,t^{i+1/2}}^2 \right) \\ & \exp \left(\Delta t \sum_{i=0}^n \frac{\beta_1^i + \beta_2^i}{1 - \Delta t(\beta_1^i + \beta_2^i)} \right). \end{aligned}$$

Proof. Applying the modified Crank-Nicolson time discretization to the semi-discrete equation (5) we get

$$\begin{aligned} & \left(\frac{u_h^{n+1} - u_h^n}{\Delta t}, v_h \right)_{t^{n+1}} + a_{SUPG}^{n+1/2} \left(\frac{u_h^{n+1} + u_h^n}{2}, v_h \right) - \int_{\Omega_{t^{n+1/2}}} \mathbf{w}_h \cdot \nabla \left(\frac{u_h^{n+1} + u_h^n}{2} \right) v_h dx \\ & = \int_{\Omega_{t^{n+1/2}}} f^{n+1/2} v_h dx + \sum_{K \in \mathcal{T}_{h,t^{n+1/2}}} \delta_K \int_K f^{n+1/2} (\mathbf{b} - \mathbf{w}_h) \cdot \nabla v_h dK. \end{aligned}$$

Testing the above equation with $v_h = (u_h^{n+1} + u_h^n)$, and using the relations

$$(u_h, u_h + v_h) = \frac{1}{2} \|u_h\|^2 + \frac{1}{2} \|u_h + v_h\|^2 - \frac{1}{2} \|v_h\|^2$$

and

$$\|u_h^n\|_{0,t^{n+1}}^2 = \|u_h^n\|_{0,t^n}^2 + \int_{t^n}^{t^{n+1}} \int_{\Omega_t} \nabla \cdot \mathbf{w}_h |u_h^n|^2 dx dt,$$

the first term can be rewritten as

$$\begin{aligned} & \int_{\Omega_{t^{n+1}}} u_h^{n+1} (u_h^{n+1} + u_h^n) dx - \int_{\Omega_{t^{n+1}}} u_h^n (u_h^{n+1} + u_h^n) dx \\ &= \frac{1}{2} \|u_h^{n+1}\|_{0,t^{n+1}}^2 + \frac{1}{2} \|u_h^{n+1} + u_h^n\|_{0,t^{n+1}}^2 - \frac{1}{2} \|u_h^n\|_{0,t^{n+1}}^2 - \frac{1}{2} \|u_h^n\|_{0,t^{n+1}}^2 \\ & \quad - \frac{1}{2} \|u_h^{n+1} + u_h^n\|_{0,t^{n+1}}^2 + \frac{1}{2} \|u_h^{n+1}\|_{0,t^{n+1}}^2 \\ &= \|u_h^{n+1}\|_{0,t^{n+1}}^2 - \|u_h^n\|_{0,t^{n+1}}^2 \\ &= \|u_h^{n+1}\|_{0,t^{n+1}}^2 - \|u_h^n\|_{0,t^n}^2 - \Delta t \int_{\Omega_{t^{n+1/2}}} \nabla \cdot \mathbf{w}_h |u_h^n|^2 dx. \end{aligned}$$

Using the above relation, the coercivity of the bilinear form and the Cauchy-Schwarz inequality for the right hand side terms, the expression can be written as

$$\begin{aligned} & \|u_h^{n+1}\|_{0,t^{n+1}}^2 - \|u_h^n\|_{0,t^n}^2 - \Delta t \int_{\Omega_{t^{n+1/2}}} \nabla \cdot \mathbf{w}_h |u_h^n|^2 dx + \frac{\Delta t}{4} \|u_h^{n+1} + u_h^n\|_{0,t^{n+1/2}}^2 \\ & \leq \frac{\Delta t}{2} \int_{\Omega_{t^{n+1/2}}} (\mathbf{w}_h \cdot \nabla (u_h^{n+1} + u_h^n)) (u_h^{n+1} + u_h^n) dx + \frac{\Delta t}{\mu} \|f^{n+1/2}\|_{0,t^{n+1/2}}^2 \\ & \quad + \frac{\mu \Delta t}{8} \|u_h^{n+1} + u_h^n\|_{0,t^{n+1/2}}^2 + \Delta t \sum_{K \in \mathcal{T}_{h,t^{n+1/2}}} \delta_K \|f^{n+1/2}\|_{0,K}^2 \\ & \quad + \frac{\Delta t}{8} \sum_{K \in \mathcal{T}_{h,t^{n+1/2}}} \delta_K \|(\mathbf{b} - \mathbf{w}_h) \cdot \nabla (u_h^{n+1} + u_h^n)\|_{0,K}^2. \end{aligned}$$

Absorbing the right hand side terms into the SUPG norm and using integration by parts for the mesh velocity term we get

$$\begin{aligned}
 & \|u_h^{n+1}\|_{0,t^{n+1}}^2 + \frac{\Delta t}{8} \| (u_h^{n+1} + u_h^n) \|_{t^{n+\frac{1}{2}}}^2 \\
 & \leq \Delta t \int_{\Omega_{t^{n+\frac{1}{2}}}} \nabla \cdot \mathbf{w}_h |u_h^n|^2 dx - \frac{\Delta t}{4} \int_{\Omega_{t^{n+\frac{1}{2}}}} \nabla \cdot \mathbf{w}_h |u_h^{n+1} + u_h^n|^2 dx \\
 & \quad + \|u_h^n\|_{0,t^n}^2 + \frac{\Delta t}{\mu} \|f^{n+\frac{1}{2}}\|_{0,t^{n+\frac{1}{2}}}^2 + \Delta t \sum_{K \in \mathcal{T}_{h,t^{n+\frac{1}{2}}}} \delta_K \|f^{n+\frac{1}{2}}\|_{0,K}^2 \\
 & \leq \Delta t \int_{\Omega_{t^{n+\frac{1}{2}}}} \nabla \cdot \mathbf{w}_h \left(|u_h^n|^2 - \frac{1}{4} |u_h^{n+1} + u_h^n|^2 \right) dx \\
 & \quad + \|u_h^n\|_{0,t^n}^2 + \frac{\Delta t}{\mu} \|f^{n+\frac{1}{2}}\|_{0,t^{n+\frac{1}{2}}}^2 + \Delta t \sum_{K \in \mathcal{T}_{h,t^{n+\frac{1}{2}}}} \delta_K \|f^{n+\frac{1}{2}}\|_{0,K}^2 \\
 & \leq \Delta t \int_{\Omega_{t^{n+\frac{1}{2}}}} \nabla \cdot \mathbf{w}_h (|u_h^n|^2 + |u_h^{n+1}|^2) dx + \|u_h^n\|_{0,t^n}^2 \\
 & \quad + \frac{\Delta t}{\mu} \|f^{n+\frac{1}{2}}\|_{0,t^{n+\frac{1}{2}}}^2 + \Delta t \sum_{K \in \mathcal{T}_{h,t^{n+\frac{1}{2}}}} \delta_K \|f^{n+\frac{1}{2}}\|_{0,K}^2.
 \end{aligned}$$

Using the ALE map and its Jacobian, the equation becomes

$$\begin{aligned}
 & \|u_h^{n+1}\|_{0,t^{n+1}}^2 + \frac{\Delta t}{4} \| (u_h^{n+1} + u_h^n) \|_{t^{n+\frac{1}{2}}}^2 \\
 & \leq \Delta t \|\nabla \cdot \mathbf{w}_h\|_{\infty,t^{n+\frac{1}{2}}} \|u_h^{n+1}\|_{0,t^{n+\frac{1}{2}}}^2 + \Delta t \|\nabla \cdot \mathbf{w}_h\|_{\infty,t^{n+\frac{1}{2}}} \|u_h^n\|_{0,t^{n+\frac{1}{2}}}^2 \\
 & \quad + \frac{\Delta t}{\mu} \|f^{n+\frac{1}{2}}\|_{0,t^{n+\frac{1}{2}}}^2 + \Delta t \sum_{K \in \mathcal{T}_{h,t^{n+\frac{1}{2}}}} \delta_K \|f^{n+\frac{1}{2}}\|_{0,K}^2.
 \end{aligned}$$

Further, with the notation

$$\begin{aligned}
 \beta_1^{n+1} &= \left\| J_{\mathcal{A}_{t_{n+1}, t_{n+\frac{1}{2}}}} \right\|_{\infty,t^{n+1}} \|\nabla \cdot \mathbf{w}_h\|_{\infty,t^{n+\frac{1}{2}}}, \\
 \beta_2^n &= \left\| J_{\mathcal{A}_{t_n, t_{n+\frac{1}{2}}}} \right\|_{\infty,t^n} \|\nabla \cdot \mathbf{w}_h\|_{\infty,t^n},
 \end{aligned}$$

the inequality turns out to be

$$\begin{aligned} & \|u_h^{n+1}\|_{0,t^{n+1}}^2 + \frac{\Delta t}{4} \| (u_h^{n+1} + u_h^n) \|_{t^{n+1/2}}^2 \\ & \leq \Delta t \beta_1^{n+1} \|u_h^{n+1}\|_{0,t^{n+1}}^2 + (1 + \Delta t \beta_2^n) \|u_h^n\|_{0,t^n}^2 \\ & \quad + \frac{\Delta t}{\mu} \|f^{n+1/2}\|_{0,t^{n+1/2}}^2 + 2\Delta t \sum_{K \in \mathcal{T}_{t^{n+1/2}}} \delta_K \|f^{n+1/2}\|_{0,K}^2. \end{aligned}$$

Summing over $i = 0, 1, 2, \dots, n$, and using the assumption on δ_k , we obtain

$$\begin{aligned} & \|u_h^{n+1}\|_{0,t^{n+1}}^2 + \frac{\Delta t}{4} \sum_{i=0}^n \| (u_h^{i+1} + u_h^i) \|_{t^{i+1/2}}^2 \\ & \leq \Delta t \beta_1^{n+1} \|u_h^{n+1}\|_{0,t^{n+1}}^2 + \Delta t \sum_{i=1}^n (\beta_1^i + \beta_2^i) \|u_h^i\|_{0,t^i}^2 \\ & \quad + (1 + \Delta t \beta_2^0) \|u_h^0\|_{0,t^0}^2 + \sum_{i=0}^n \left(\frac{\Delta t}{\mu} \|f^{i+1/2}\|_{0,t^{i+1/2}}^2 + \frac{\Delta t^2}{2} \|f^{i+1/2}\|_K^2 \right) \\ & \leq \Delta t \sum_{i=1}^{n+1} (\beta_1^i + \beta_2^i) \|u_h^i\|_{0,t^i}^2 + (1 + \Delta t \beta_2^0) \|u_h^0\|_{0,t^0}^2 \\ & \quad + \Delta t \sum_{i=0}^n \left(\frac{2}{\mu} + \frac{\Delta t}{2} \right) \|f^{i+1/2}\|_{0,t^{i+1/2}}^2. \end{aligned}$$

Finally, using Grownwall's lemma, we get

$$\begin{aligned} & \|u_h^{n+1}\|_{0,t^{n+1}}^2 + \frac{\Delta t}{4} \sum_{i=0}^n \| (u_h^{i+1} + u_h^i) \|_{t^{i+1/2}}^2 \\ & \leq \left((1 + \Delta t \beta_2^0) \|u_h^0\|_{0,t^0}^2 + \Delta t \sum_{i=0}^n \left(\frac{2}{\mu} + \Delta t \right) \|f^{i+1/2}\|_{0,t^{i+1/2}}^2 \right) \\ & \quad \exp \left(\Delta t \sum_{i=1}^{n+1} \frac{\beta_1^i + \beta_2^i}{1 - \Delta t (\beta_1^i + \beta_2^i)} \right). \end{aligned}$$

The estimate is stable provided we have

$$\Delta t < \frac{1}{\beta_1^n + \beta_2^n} = \left(\left\| J_{\mathcal{A}_{t_n, t_{n-1/2}}} \right\|_{\infty, t^n} \|\nabla \cdot \mathbf{w}_h\|_{\infty, t^{n-1/2}} + \left\| J_{\mathcal{A}_{t_n, t_{n+1/2}}} \right\|_{\infty, t^n} \|\nabla \cdot \mathbf{w}_h\|_{\infty, t_{n+1/2}} \right)^{-1}.$$

Thus, the scheme is only conditionally stable with the time step restriction given above. \square

3.3 Discrete ALE-SUPG with backward-difference (BDF2) time discretization

We now consider the backward difference method of order two for temporal discretization. For the equation (3.3), the backward-difference method gives

$$\frac{3}{2}u^{n+1} - 2u^n + \frac{1}{2}u^{n-1} = \Delta t f(u^{n+1}, t^{n+1}).$$

Lemma 5. Stability estimates for the non-conservative ALE-SUPG form applying backward-difference formula: *Let the discrete version of (2.8) and assumption (2.9) on δ_K hold true. Further, assume $\delta_K \leq \frac{\Delta t}{4}$. Then the solution satisfies*

$$\begin{aligned} & \|u_h^{n+1}\|_{0, t^{n+1}}^2 + \|2u_h^{n+1} - u_h^n\|_{0, t^n}^2 + \Delta t \sum_{i=1}^{n+1} \|u_h^i(t)\|_{t^i}^2 \leq \\ & \leq \left((1 + \Delta t \alpha_2^0) \|u_h^0\|_{0, t^0}^2 + \|2u_h^1 - u_h^0\|_{0, t^1}^2 + \Delta t \sum_{i=1}^{n+1} \left(\frac{2}{\mu} + \frac{\Delta t}{2} \right) \|f^i\|_{0, t^i}^2 \right) \\ & \quad \exp \left(\Delta t \sum_{i=1}^{n+1} \frac{2\alpha_1^i + \alpha_2^i}{1 - \Delta t(2\alpha_1^i + \alpha_2^i)} \right). \end{aligned}$$

Proof. Applying the backward difference temporal discretization to the

semi-discrete equation (5) with the test function u_h^{n+1} , we get

$$\begin{aligned} & \left(\frac{3}{2}u_h^{n+1} - 2u_h^n + \frac{1}{2}u_h^{n-1}, u_h^{n+1} \right)_{\Omega_{t^{n+1}}} + \Delta t a_{SUPG}^{n+1}(u_h^{n+1}, u_h^{n+1})_t \\ & - \frac{\Delta t}{2} \int_{\Omega_{t^{n+1}}} \mathbf{w}_h^{n+1} \cdot \nabla((u_h^{n+1})^2) dx = \Delta t \int_{\Omega_{t^{n+1}}} f^{n+1} u_h^{n+1} dx \\ & + \Delta t \sum_{K \in \mathcal{T}_{t^{n+1}}} \delta_K \int_K f^{n+1} (\mathbf{b} - \mathbf{w}_h^{n+1}) \cdot \nabla u_h^{n+1} dK. \end{aligned}$$

The first term can be written as

$$\begin{aligned} & \left(\frac{3}{2}u_h^{n+1} - 2u_h^n + \frac{1}{2}u_h^{n-1}, u_h^{n+1} \right)_{\Omega_{t^{n+1}}} = \frac{1}{4} \left(\|u_h^{n+1}\|_{0,t^{n+1}}^2 - \|u_h^n\|_{0,t^n}^2 \right. \\ & + \|2u_h^{n+1} - u_h^n\|_{0,t^{n+1}}^2 - \|2u_h^n - u_h^{n-1}\|_{0,t^n}^2 + \|u_h^{n+1} - 2u_h^n + u_h^{n-1}\|_{0,t^{n+1}}^2 \\ & \left. + \int_{t^n}^{t^{n+1}} \int_{\Omega_t} \nabla \cdot \mathbf{w}_h^{n+1}(t) \left[(u_h^n)^2 + (u_h^n - u_h^{n-1})^2 \right] \right). \end{aligned} \quad (3.4)$$

We substitute equation (3.4) for the first term and use the same estimates as we worked out in previous sections so that the fully discrete equation becomes

$$\begin{aligned} & \frac{1}{4} \left(\|u_h^{n+1}\|_{0,t^{n+1}}^2 + \|2u_h^{n+1} - u_h^n\|_{0,t^{n+1}}^2 + \|u_h^{n+1} - 2u_h^n + u_h^{n-1}\|_{0,t^{n+1}}^2 \right) \\ & + \frac{\Delta t}{4} \|u_h^{n+1}\|_{t^{n+1}}^2 \leq \frac{1}{4} \left(\|u_h^n\|_{0,t^n}^2 + \|2u_h^n - u_h^{n-1}\|_{0,t^n}^2 \right) \\ & + \frac{1}{4} \int_{t^n}^{t^{n+1}} \int_{\Omega_t} \nabla \cdot \mathbf{w}_h^{n+1}(t) \left[(u_h^n)^2 + (u_h^n - u_h^{n-1})^2 \right] + \frac{2\Delta t}{\mu} \|f^{n+1}\|_{0,t^{n+1}}^2 \\ & + \frac{\Delta t}{2} \|\nabla \cdot \mathbf{w}_h^{n+1}\|_{\infty,t^{n+1}} \|u_h^{n+1}\|_{0,t^{n+1}}^2 + 2\Delta t \sum_{K \in \mathcal{T}_{t^{n+1}}} \delta_K \|f^{n+1}\|_K^2. \end{aligned}$$

Summing over $i = 0, 1, 2, \dots, n$, and with the same notations as in the

implicit Euler case, we get

$$\begin{aligned}
 & \|u_h^{n+1}\|_{0,t^{n+1}}^2 + \|2u_h^{n+1} - u_h^n\|_{0,t^{n+1}}^2 + \|u_h^{n+1} - 2u_h^n + u_h^{n-1}\|_{0,t^{n+1}}^2 \\
 & + \Delta t \sum_{i=0}^n \|u_h^{i+1}\|_{t^{i+1}}^2 \leq 2\Delta t \alpha_1^{n+1} \|u_h^{n+1}\|_{0,t^{n+1}}^2 + \|u_h^0\|_{0,t^0}^2 + \|2u_h^1 - u_h^0\|_{0,t^1}^2 \\
 & + \Delta t \alpha_2^0 \|u_h^0\|_{0,t^0}^2 + \Delta t \sum_{i=1}^n (2\alpha_1^i + \alpha_2^i) \|u_h^i\|_{0,t^i}^2 \\
 & + 4\Delta t \sum_{i=1}^n \left(\frac{2}{\mu} + \frac{\Delta t}{2} \right) \|f^{i+1}\|_{0,t^{i+1}}^2 \\
 & \leq (1 + \Delta t \alpha_2^0) \|u_h^0\|_{0,t^0}^2 + \|2u_h^1 - u_h^0\|_{0,t^1}^2 + \Delta t \sum_{i=1}^{n+1} (2\alpha_1^i + \alpha_2^i) \|u_h^i\|_{0,t^i}^2 \\
 & \quad + 4\Delta t \sum_{i=1}^{n+1} \left(\frac{2}{\mu} + \frac{\Delta t}{2} \right) \|f^i\|_{0,t^i}^2.
 \end{aligned}$$

By using Grownwall's lemma we get the stability estimate provided we have

$$\Delta t < \frac{1}{\sup_{n \in [0, N]} (2\alpha_1^n + \alpha_2^n)}.$$

Here, we can see the stability estimate is again only conditionally stable with the time step restriction depending on the ALE map. \square

4 Numerical results

Numerical results obtained with the proposed numerical scheme for the considered model problem are presented in this section. We first consider a standard example without convection and compare the standard Galerkin solutions with different time steps Δt and the SUPG solution with varying δ_0 , which is a numerical parameter in $\delta_K (= \delta_0 h_{K,t} / |\mathbf{w}|_{\infty,t})$. We next consider a PDE in a time-dependent domain with boundary and interior layers. In this example, we study the influence of different time

discretizations on the stabilized solution of the PDE. The system of matrix resulting from the considered numerical scheme is solved by using the direct solver UMFPACK [17]. All computations are performed using our in-house finite element package, ParMoon, see [18] for more details.

The piecewise quadratic finite elements are used for the spatial discretization. The first order backward Euler, the second order Crank-Nicolson, and the backward-difference(BDF2) are used for the temporal discretization. Numerical solutions obtained with the standard Galerkin and the SUPG method are presented.

4.1 Example 1

The purpose of this example is to study the influence of the time-step, Δt , the stabilization parameter, δ_0 , on the stabilized ALE solution obtained with different time-discretization methods. Moreover, we consider a problem with zero convection. Nevertheless, the ALE formulation introduces a convective mesh velocity in the PDE, see equation (2.2). Therefore, the effects of the SUPG stabilization depend solely on the mesh movement.

Let the scalar time-dependent equation be

$$\begin{aligned} \frac{\partial u}{\partial t} - \epsilon \Delta u &= 0 && \text{in } \Omega_t \times (0, T], \\ u &= 0 && \text{on } \partial\Omega_t \times [0, T], \\ u|_{t=0} &= 1600 Y_1(1 - Y_1) Y_2(1 - Y_2) && \text{in } \Omega_0, \end{aligned}$$

where $\epsilon = 0.01$ and $\Omega_0 = (0, 1)^2$ is the initial (reference) domain, $\hat{\Omega}$. Further, the position of the time-dependent domain $x \in \Omega_t$ at time t is ruled by

$$x(Y, t) = \mathcal{A}_t(Y) \text{ such that } \begin{cases} x_1 = Y_1(2 - \cos(20\pi t)) \\ x_2 = Y_2(2 - \cos(20\pi t)), \end{cases} \quad (Y_1, Y_2) \in \hat{\Omega}.$$

In computations, the piecewise linear interpolation in time is used to obtain the new position of the domain, that is, $x(Y, s) \in \Omega_s$ for $s \in$

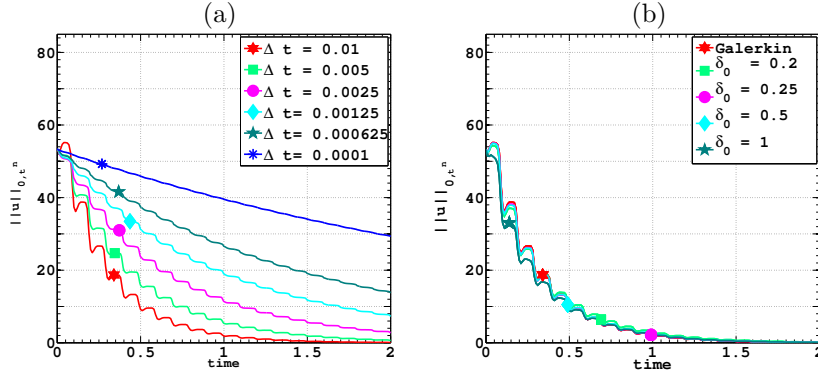


Figure 1: L^2 -norm of the solution obtained with implicit Euler time discretization, (a) Galerkin solution with different time-steps Δt , (b) SUPG solution for $\Delta t = 0.01$ with different stabilization parameters δ_0 .

$[t^n, t^{n+1}]$ given by

$$x(Y, s) = \frac{s - t^n}{\Delta t} x(Y, t^{n+1}) + \frac{t^{n+1} - s}{\Delta t} x(Y, t^n).$$

Hence, the domain velocity is obtained as

$$\mathbf{w}(Y, s) = \frac{x(Y, t^{n+1}) - x(Y, t^n)}{\Delta t}.$$

For the considered displacement, the square domain will expand and shrink over a period of time, but the origin will remain intact.

We triangulate the square domain with 8,192 triangles. Further, piecewise linear finite elements P_1 are used for the spatial discretization, which results in 4,225 degrees of freedom (dof). The standard Galerkin and the SUPG solutions obtained with the backward Euler time discretization for different Δt and δ_0 with $\Delta t = 0.01$, respectively, are depicted in Figure 1. As expected, the backward Euler solution is

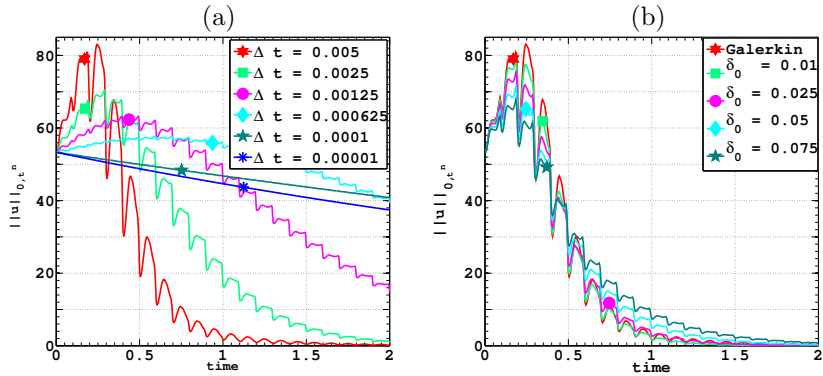


Figure 2: L^2 -norm of the solution obtained with Crank-Nicolson time discretization, (a) Galerkin solution with different time-steps Δt , (b) SUPG solution for $\Delta t = 0.005$ with different stabilization parameters δ_0 .

more diffusive and the diffusivity effect reduces when the time step is reduced, see Figure 1 (a). In addition to the diffusivity effect, a periodic oscillation in the solution due to the mesh movement is observed when the time step is large. These oscillations reduce with smaller time steps, and the solution becomes monotone. This behavior supports our stability analysis that the time step depends on the mesh velocity, see Lemma 3. Figure 1 (b) presents the SUPG solutions for different δ_0 , where the oscillatory case $\Delta t = 0.01$ from Figure 1 (a) is considered. This parametric study is performed in order to see the effects of SUPG discretization. Though the Euler solution is already more diffusive, the artificial diffusive effect of SUPG is not observed with the chosen time step $\Delta t = 0.01$. Since piecewise linear finite elements are used, SUPG induces diffusion only in the streamline (mesh velocity) direction.

Next, the standard Galerkin and the SUPG solutions obtained with the Crank-Nicolson time discretization for different Δt and δ_0 with $\Delta t =$

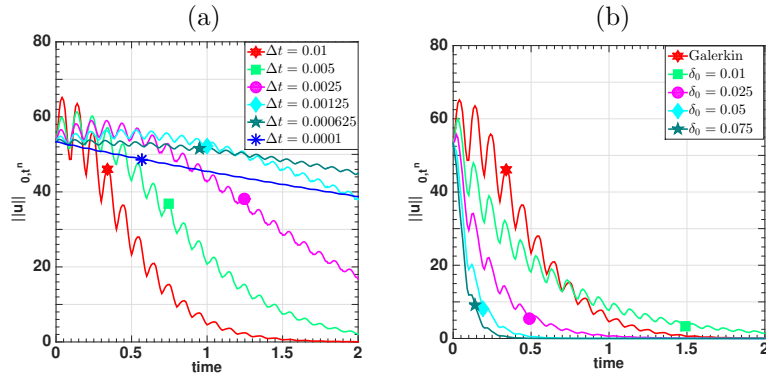


Figure 3: L^2 -norm of the solution obtained with backward difference time discretization (BDF2), (a) Galerkin solution with different time-steps Δt , (b) SUPG solution for $\Delta t = 0.01$ with different stabilization parameters δ_0 .

0.005, respectively, are depicted in Figure 2. Recall that the Crank-Nicolson method is only A -stable and not strongly A -stable even in a stationary domain. In addition, the time step depends on the mesh velocity, see Lemma 4. Thus the influence of the mesh velocity is very high in the Crank-Nicolson solution, especially when Δt is large, see Figure 2 (a). The Galerkin solution is oscillatory except for the cases $\Delta t = 0.0001$ and $\Delta t = 0.00001$. The reason for high oscillations in the Crank-Nicolson method can be due to the assembling of the stiffness matrix on the $\Omega_{t^{n+1/2}}$ domain, which induces more numerical error. Further, the SUPG discretization suppresses the oscillations when the value of δ_0 is increased. More interestingly, the SUPG solution become less diffusive compared to the Galerkin solution, see Figure 2 (b).

Finally, the backward-difference (BDF2) solution with the standard Galerkin and the SUPG discretizations for different Δt and δ_0 with $\Delta t = 0.01$, respectively, are depicted in Figure 3. Though there are

oscillations in the BDF2 solution due to the mesh velocity, oscillations are less, compared to the Crank-Nicolson solution, see Figure 3 (a) and Figure 2 (a). Moreover, the influence of the SUPG parameter is very high and the solutions become more diffusive, see Figure 3 (b), when the value of δ_0 is increased, which is the inherent property of the SUPG discretization.

4.2 Example 2

The purpose of this example is to study the effect of different time discretizations and the ALE formulations (conservative, non-conservative ALE forms) on the SUPG solution of advection dominated PDEs in time-dependent domain. Thus, a typical fluid-structure interaction (FSI) problem, in which a flow passing through a rectangular structure (beam) that deforms with time, is considered. A predefined adaptive mesh with high resolution in the vicinity of the deforming structure is considered. Nevertheless, the mesh away from the structure is comparatively coarser.

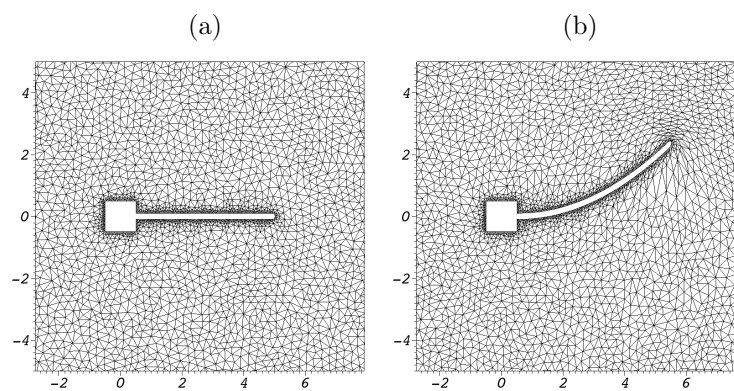


Figure 4: *The schematic diagram of the domain with unstructured triangular mesh as illustrated in Example 2. (a) Beam at the initial position and (b) beam at its maximum amplitude.*

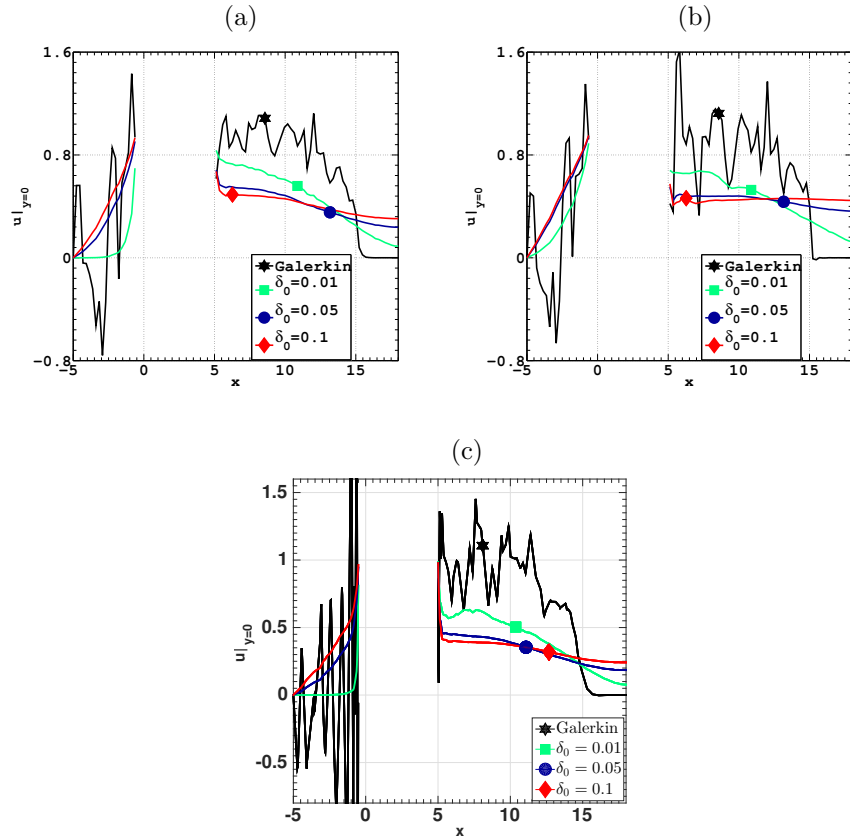


Figure 5: Galerkin and SUPG solutions with different values of δ_0 over the line $y = 0$ in Example 2. (a) Implicit Euler, (b) Crank-Nicolson, and (c) backward difference (BDF2).

Further, the tip of the beam is considered to be semi-circular to do away with the singularities that might occur due to the sharp corners. Let

$$\Omega_0^S = \{(-0.5, 0.5) \times (-0.5, 0.5)\} \cup \{(0.5, 4.5) \times (-0.03, 0.03)\}$$

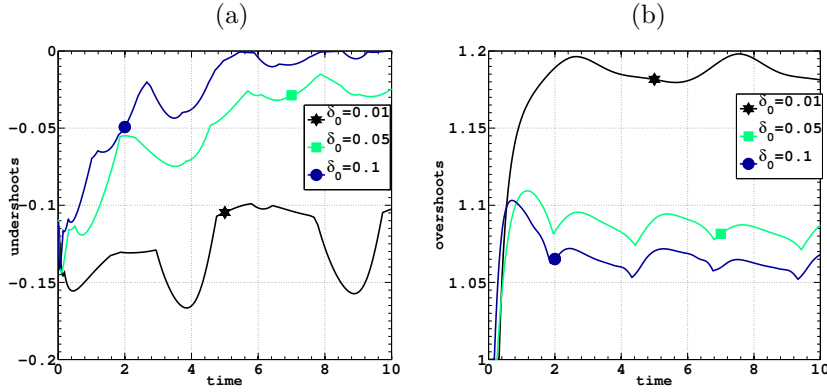


Figure 6: The observed undershoots/overshoots with implicit Euler time discretization in the SUPG solution for different values of δ_0 : (a) undershoots and (b) overshoots.

be the rectangular structure (beam) at time $t = 0$. The two-dimensional channel that excludes the beam Ω_0^S is defined by

$$\Omega_0 = \{(-5, 18) \times (-5, 5)\} \setminus \bar{\Omega}_0^S.$$

Further, we define $\Gamma_D = \{-5\} \times (-5, 5)$ as the Dirichlet boundary and $\Gamma_N = \partial\Omega_t \setminus \Gamma_D$ as the Neumann boundary. Moreover, we consider the initial domain as the reference domain for the ALE mapping, that is, $\hat{\Omega} = \Omega_0$. Now, the coordinates of the point in time-dependent domain $(x_1, x_2) \in \Omega_t$ are defined by

$$x(Y, t) = \mathcal{A}_t(Y) \begin{cases} x_1 = Y_1 + 0.05(0.25 d \tan \theta - Y_2 \sin \theta) \\ x_2 = Y_2 + 0.05d, \end{cases} \quad (Y_1, Y_2) \in \hat{\Omega},$$

where the sinusoidal movement of the beam is prescribed by

$$d = 0.75(x_1 - 0.5)^2 \sin(2\pi t/5), \quad \theta = \tan^{-1} \left(\frac{x_2}{x_1 - 0.5} \right).$$

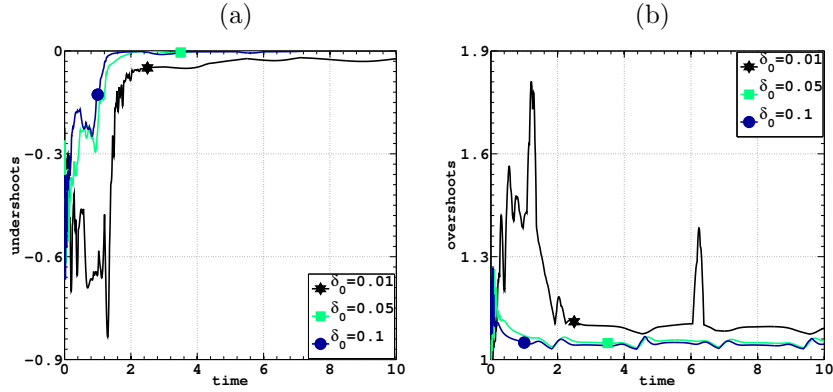


Figure 7: The observed undershoots/overshoots with Crank-Nicolson time discretization in the SUPG solution for different values of δ_0 : (a) undershoots and (b) overshoots.

We now solve a scalar (energy) equation

$$\frac{\partial u}{\partial t} - \epsilon \Delta u + \mathbf{b} \cdot \nabla u = 0, \quad \text{in } \Omega_t \times (0, T],$$

with $\epsilon = 10^{-6}$ and $\mathbf{b}(x_1, x_2) = (1, 0)^T$. Further, we impose the homogeneous Neumann condition on Γ_N , and set

$$u_D(x_1, x_2) = \begin{cases} 1 & \text{on } \partial\Omega_t^S, \\ 0 & \text{else,} \end{cases}$$

on the Dirichlet boundary. Boundary and interior layers in the vicinity and the wake region, respectively, of the solid beam will occur due to a small diffusive constant. Since the solid beam deforms (up and down) periodically, the position of the boundary and the interior layers will also change with time. The computations are performed up to the dimensionless time $T = 10$ with a time step $\Delta t = 0.01$. Further, an elastic-solid

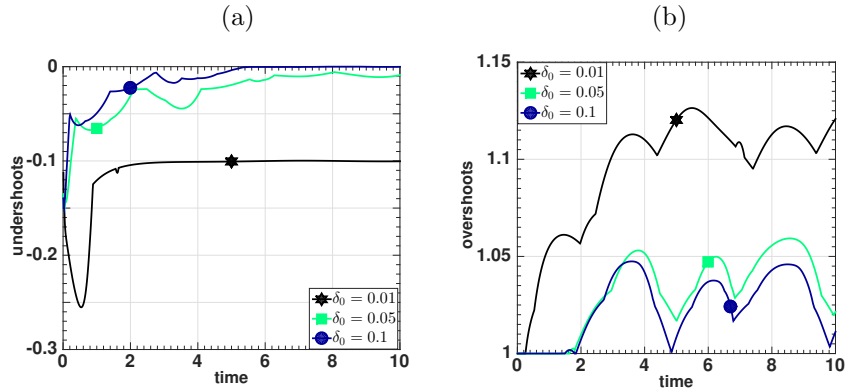


Figure 8: The observed undershoots/overshoots with backward difference time discretization in the SUPG solution for different values of δ_0 : (a) undershoots and (b) overshoots.

mesh update technique is used to handle the mesh movement. At each time step, we first compute the displacement of the beam and then solve the linear elastic equation in Ω_{t^n} to compute the inner points displacement by considering the displacement on $\partial\Omega_{t^{n+1}}^S$ as the Dirichlet value. This elastic update technique avoids the re-meshing during the entire simulation, see Figure 4.

In order to understand the behavior of the Galerkin and SUPG solutions with different values of δ_0 , numerical solutions at the middle of the channel, that is, at $y = 0$, are depicted in Figure 5 for different time discretizations. As expected, the Galerkin solutions obtained with (a) implicit Euler, (b) Crank-Nicolson, and (c) backward difference (BDF2) discretizations contain spurious oscillations and instabilities, see the Galerkin solutions in Figure 5, whereas the oscillations are suppressed in the SUPG solution. Moreover, the boundary layer is approximated sharply by any smaller value of δ_0 .

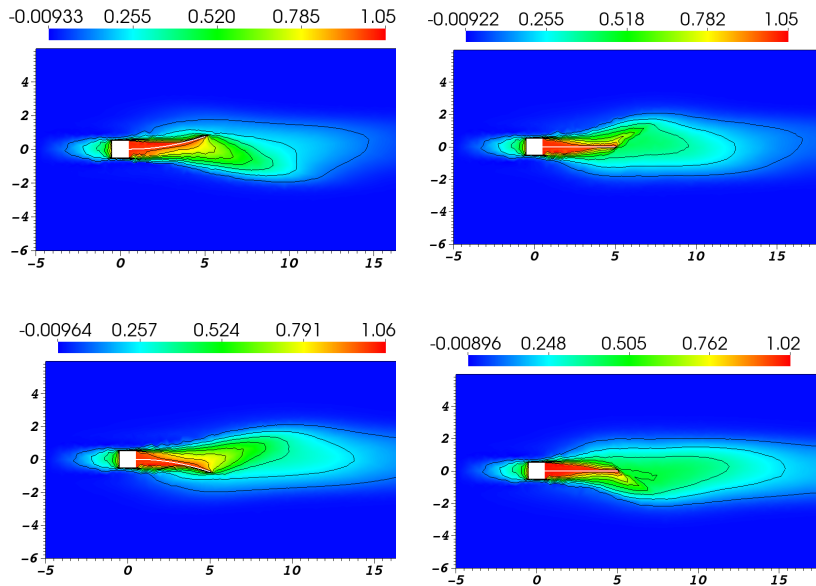


Figure 9: The sequence of solutions obtained with the SUPG $\delta_0 = 0.05$ method for implicit Euler time discretization at different instances $t = 6.3, 7.5, 8.8, 10$.

Next, to get an insight into the robustness and effectiveness of the SUPG stabilization, the undershoots and the overshoots in the SUPG solution for different values of δ_0 are examined in this example. An array of computations with (i) $\delta_0 = 0.01$, (ii) $\delta_0 = 0.05$, and (iii) $\delta_0 = 0.1$ are performed, and the results are presented in Figure 6, 7, and 8. We can observe that the undershoots and overshoots are lesser in the implicit Euler method than the other Crank-Nicolson, and backward-difference schemes at the initial period of time until $t = 2$ (note that the scaling of figures are different). Though the oscillations in the SUPG solution obtained with the Crank-Nicolson scheme are more frequent at the initial

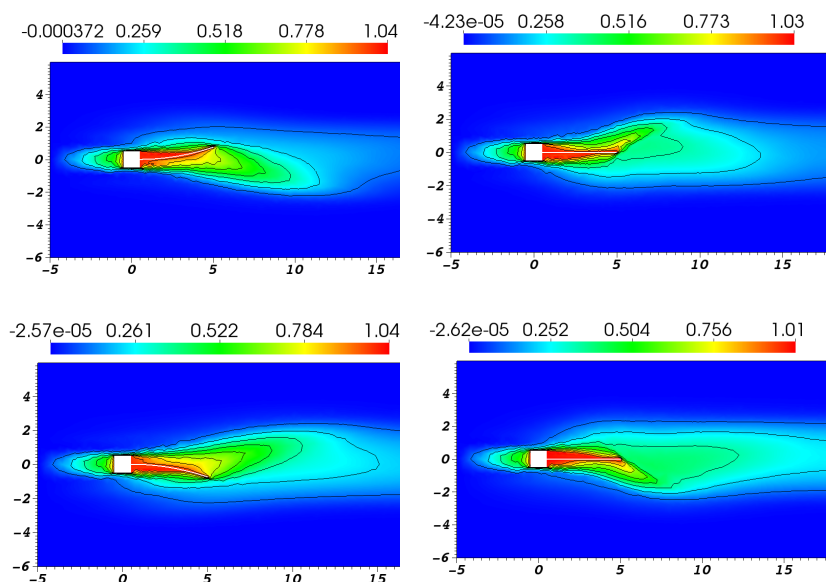


Figure 10: The sequence of solutions obtained with the SUPG $\delta_0 = 0.05$ method for Crank-Nicolson time discretization at different instances $t = 6.3, 7.5, 8.8, 10$.

stage, for us until $t = 2$, the undershoots and overshoots at the later stage are minimum compared to the other two cases, see Figure 7. Further, the undershoots and overshoots in the SUPG solutions with $\delta_0 = 0.05$ and (ii) $\delta_0 = 0.1$ are similar in all time discretizations. Nevertheless, a smaller value of δ_0 is preferred in order to avoid the smearing effect, which will be discussed next.

Though the SUPG approximation almost suppressed the spurious oscillations in the numerical solution, there are very small overshoots and undershoots (around 10%) for the chosen $\delta_0 = 0.05$. One could reduce these undershoots and overshoots by increasing the value of δ_0 further.

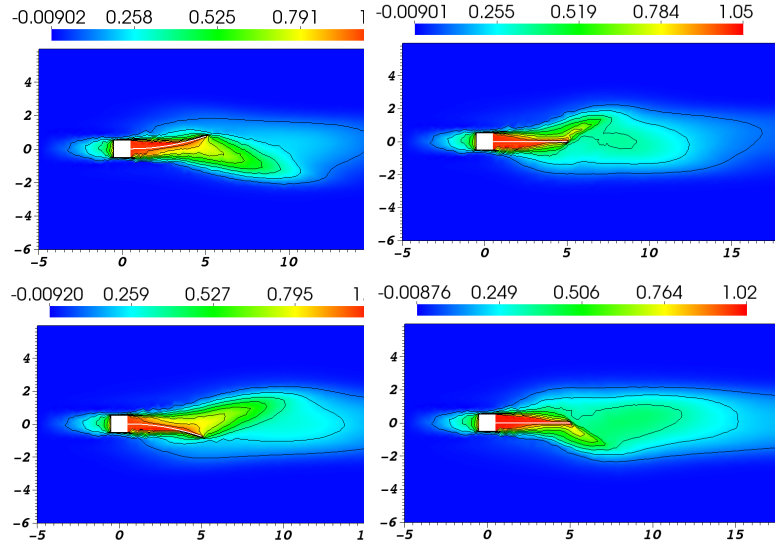


Figure 11: The sequence of solutions obtained with the SUPG $\delta_0 = 0.05$ method for backward difference time discretization at different instances $t = 6.3, 7.5, 8.8, 10$.

However, it will smear the solution. This is a well-known behavior of the SUPG method in stationary domains. Thus, the optimal choice of the stabilization parameter varies with numerical examples, and it is an open problem, see [20]. Plots in Figure 5 show the smearing effect of the boundary layer. In order to see the smearing effect in the entire domain, a sequence of SUPG solution profiles obtained with $\delta_0 = 0.05$ at different instances $t = 6.3, 7.5, 8.8, 10$ are depicted in Figures 9, 10, and 11. In these plots, the range of values in the caption for the respective time instances among all time discretizations is kept the same for better comparison. We can observe from these plots that the solutions obtained with the backward Euler and BDF2 discretizations are more diffusive

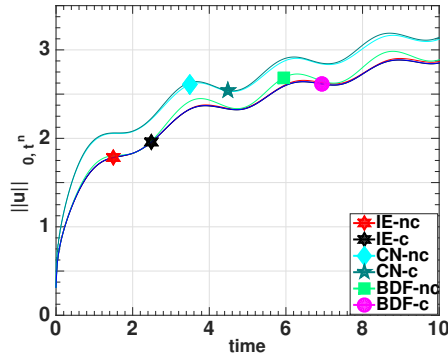


Figure 12: The L^2 -norm of the solution for Example 2 with all the time discretizations for both the conservative and non-conservative case.

than the solution of the Crank-Nicolson discretization.

Finally, to study quantitatively the stabilization effects on the solution, the variation in the total energy of the system over the period of time in different time discretizations are plotted in Figure 12. In addition to different discretizations, solutions obtained with both the conservative and the non-conservative ALE forms are also compared in Figure 12.

Since the backward Euler and BDF2 solutions are more diffusive than the Crank-Nicolson solution, the total energy in the system is slightly less due to the homogeneous Dirichlet boundary condition on the side wall. Nevertheless the variation is very small (≈ 0.2). More interestingly, the difference between the conservative and the non-conservative solutions obtained with different time discretization is negligible in this numerical example. Note that the domain velocity is not very high in this particular example. Therefore, either the conservative or non-conservative scheme can be used. The non-conservative is preferred for domains with small deformation, since a reaction type mesh velocity term and the GCL condition can be avoided.

5 Summary

The ALE-SUPG finite element scheme for convection dominated transient convection-diffusion equation in time-dependent domains is presented in this paper. Further, the influence of the backward Euler, the Crank-Nicolson, and the backward difference (BDF2) temporal discretizations on the solution of the non-conservative ALE-SUPG finite element method is investigated. It is observed that the Crank-Nicolson scheme induces high oscillations in the numerical solution compared to the implicit Euler and the backward difference time discretizations. Further, the difference between the solutions obtained with the conservative and non-conservative ALE forms highly depends on the deformation of the domain. The difference is significant when the deformation of the domain is large, whereas it is negligible in domains with small deformation. Since the deformation in most of the FSI problems is moderate, as the volume of the domain does not vary too much and the divergence of mesh velocity calculation can be avoided, the non-conservative ALE form is preferred. Next, the influence of the SUPG stabilization parameter on the solution is presented. It is observed that the Crank-Nicolson scheme is less dissipative than the implicit Euler and the backward difference method. Moreover, the backward difference scheme is more sensitive to the stabilization parameter δ_k than the other time discretizations.

This work was partially supported by the IISc Mathematics Initiative (IMI) at Indian Institute of Science, Bangalore and by Council of Scientific and Industrial Research (CSIR), India.

References

- [1] A. N. Brooks, T. J. R. Hughes, *Streamline upwind/Petrov-Galerkin formulations for convection dominated flows with particular emphasis on the incompressible Navier-Stokes equations*, Comput. Methods Appl. Mech. Eng., 32, 1982, 199–259.

- [2] D. Boffi, L. Gastaldi, *Stability and geometric conservation laws for ALE formulations*, Comp. Meth. in App. Mech. and Engg, 193, 2004, 4717–4739.
- [3] E. Burman, *Consistent SUPG method for transient transport problems: Stability and convergence*, Comput. Methods in Appl. Mech. and Engrg, 199, 2010, 1114–1123.
- [4] E. Burman, A. Ern, *Continuous interior penalty hp-finite element methods for advection and advection-diffusion equations*, Math. Comp, 76, 2007, 1119–1140.
- [5] E. Burman, P. Hansbo, *Edge stabilization for Galerkin approximations of convection-diffusion-reaction problems*, Comput. Methods Appl. Mech. Eng., 193, 2004, 1437–1453.
- [6] F. Nobile, *Numerical approximation of fluid-structure interaction problems with application to haemodynamics*, École Polytechnique Fédérale de Lausanne, PhD thesis, 2001.
- [7] G. Matthies, P. Skrzypacz, L. Tobiska, *A unified convergence analysis for local projection stabilisations applied to the Oseen problem*, Math. Model. Numer. Anal., 41, 2007, 713–742.
- [8] J.L. Guermond, *Stabilization of Galerkin approximations of transport equations by subgrid modeling*, ESAIM: Math. Model. Numer. Anal., 33, 1999, 1293–1316.
- [9] J. A. Mackenzie, W. R. Mekwi, *An unconditionally stable second-order accurate ALEFEM scheme for two dimensional convection-diffusion problems*, IMA J Numer Anal., 2012.
- [10] L. Franca, S. Frey, T. Hughes, *Stabilized finite element methods: I. Application to the advective-diffusive model*, Comput. Methods Appl. Mech. Engrg., 32, 1992, 888–905.

- [11] M. Braack, E. Burman, *Local projection stabilization for the Oseen problem and its interpretation as a variational multiscale method*, SIAM J. Numer. Anal., 43, 2006, 2544-2566.
- [12] R. Codina, *Stabilization of incompressibility and convection through orthogonal subscales in finite element methods*, Comput. Methods Appl. Mech. Eng. 190, 2000, 1579–1599.
- [13] R. Codina, *Comparison of some finite element methods for solving the diffusion-convection-reaction equation*, Comput. Methods Appl. Mech. Eng., 156, 1998, 185–210.
- [14] S. Ganesan, S. Srivastava, *ALE-SUPG finite element method for convection-diffusion problems in time-dependent domains: Conservative form* Appl. Math. and Comp., 303, 2017, 128-145.
- [15] T. Tezduyar, D. Ganjoo, *Petrov Galerkin formulations with weighting functions dependent upon spatial and temporal discretization: applications to transient convection-diffusion problems*, Comput. Methods Appl. Mech. Engrg., 59, 1986, 49-71.
- [16] T. E. Tezduyar, Y. Osawa, *Finite element stabilization parameters computed from element matrices and vectors*, Comput. Methods Appl. Mech. Engrg., 2000, 411-430.
- [17] T. A. Davis, *Algorithm 832: UMFPACK V 4.3—an unsymmetric-pattern multifrontal method*, ACM Trans. Math. Software, 30, 2004, 196–199.
- [18] U. Wilbrandt, C. Bartsch, N. Ahmed, N. Alia, F. Anker, L. Blank, A. Caiazzo, S. Ganesan, S. Giere, G. Matthies, R. Meesala, A. Shamim, J. Venkatesan, V. John, *ParMoon - a modernized program package based on mapped finite elements*, Computers and Mathematics with Applications, 74, 2016, 74-88.
- [19] V. John, J. Novo, *Error analysis of the SUPG finite element discretization of evolutionary convection-diffusion- reaction equations*, SIAM J. Numer. Anal., 49, 2011, 1149–1176.

Shweta Srivastava, Sashikumaar Ganesan

- [20] V. John, P. Knobloch, *Adaptive computation of parameters in stabilized methods for convection-diffusion problems*, Numerical Mathematics and Advanced Applications, 2011, 275–283.

Resumen: El presente artículo desarrolla el análisis numérico de una ecuación escalar con convección dominada y distintas discretizaciones temporales en dominios dependientes del tiempo. Para la discretización temporal se hará uso de los métodos en reversa de Euler, el de Crank-Nicolson y otros métodos de diferencias finitas en reversa. El dominio dependiente del tiempo es tratado desde un enfoque lagrangiano-euleriano arbitrario (ALE). Particularmente, consideramos la forma no conservativa del enfoque ALE. Además, empleamos el método de Petrov-Galerkin (SUPG) para discretización espacial. Se prueba que la estabilidad de la solución completamente discreta, independiente de la discretización temporal, es solo condicionalmente estable. Además, se estudia la dependencia de la solución numérica respecto al parámetro estabilizador δ_k . Se corrobora que el esquema Crank-Nicolson es menos disipativo que el método implícito de Euler y el método de diferencias en reversa. Más aun, el esquema de diferencias en reversa resulta más sensible al parámetro estabilizador δ_k que otras discretizaciones temporales.

Palabras clave: Ecuación reacción-convección-difusión, estabilización SUPG, ley de conservación geométrica (GCL), dominio dependiente del tiempo, enfoque lagrangiano-euleriano arbitrario, discretizaciones temporales.

Shweta Srivastava
IISc Mathematics Initiative (IMI),
Department of Mathematics
Indian Institute of Science (IISc), Bangalore,
India
shweta@imca.edu.pe

Sashikumaar Ganesan
Department of Computational and Data Sciences,
Indian Institute of Science (IISc), Bangalore,
India
sashi@cds.iisc.ac.in